MICROCOPY RESOLUTION TEST CHART

NATIONAL BUREAU OF STANDARDS-1963-A

AFWAL-TR-83-4157

(12)

OBSERVATION OF OXIDE SKIN IN
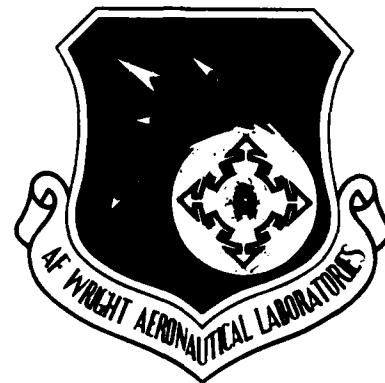POWDER METALLURGY ALUMINUM ALLOYS

Gunter Staniek
Structural Metals Branch

March 1984

Final Report for Period December 1981 – December 1982

DTIC
ELECTE
SEP 2 6 1984
S   D
B

04   13

NOTICE

When Government drawings, specifications, or other data are used for any purpose other than in connection with a definitely related Government procurement operation, the United States Government thereby incurs no responsibility nor any obligation whatsoever; and the fact that the government may have formulated, furnished, or in any way supplied the said drawings, specifications, or other data, is not to be regarded by implication or otherwise as in any manner licensing the holder or any other person or corporation, or conveying any rights or permission to manufacture use, or sell any patented invention that may in any way be related thereto.

This report has been reviewed by the Office of Public Affairs (ASD/PA) and is releasable to the National Technical Information Service (NTIS). At NTIS, it will be available to the general public, including foreign nations.

This technical report has been reviewed and is approved for publication.

FRANCIS H. FROES, TECHNICAL AREA MANAGER,
TITANIUM GROUP
STRUCTURAL METALS BRANCH
METALS & CERAMICS DIVISION

FOR THE COMMANDER

GAIL E. EICHELMAN
CHIEF, STRUCTURAL METALS BRANCH
METALS & CERAMICS DIVISION

"If your address has changed, if you wish to be removed from our mailing list, or if the addressee is no longer employed by your organization please notify MLLS , W-PAFB, OH 45433 to help us maintain a current mailing list".

Copies of this report should not be returned unless return is required by security considerations, contractual obligations, or notice on a specific document.

REPORT DOCUMENTATION PAGE		READ INSTRUCTIONS BEFORE COMPLETING FORM
1. REPORT NUMBER AFWAL-TR-83-4157	2. GOVT ACCESSION NO. AD-A145919	3. RECIPIENT'S CATALOG NUMBER
4. TITLE (and Subtitle) OBSERVATION OF OXIDE SKIN IN POWDER METALLURGY ALUMINUM ALLOYS		5. TYPE OF REPORT & PERIOD COVERED Final Report for Period December 1981-December 1982
		6. PERFORMING ORG. REPORT NUMBER
7. AUTHOR(s) Gunter Staniek		8. CONTRACT OR GRANT NUMBER(s)
9. PERFORMING ORGANIZATION NAME AND ADDRESS Materials Laboratory (MLLS) AF Wright Aeronautical Laboratories, AFSC Wright-Patterson Air Force Base, Ohio 45433		10. PROGRAM ELEMENT, PROJECT, TASK AREA & WORK UNIT NUMBERS P.E. 62102F 24180207
11. CONTROLLING OFFICE NAME AND ADDRESS Materials Laboratory (MLLS) AF Wright Aeronautical Laboratories, AFSC Wright-Patterson Air Force Base, Ohio 45433		12. REPORT DATE March 1984
		13. NUMBER OF PAGES 50
14. MONITORING AGENCY NAME & ADDRESS(If different from Controlling Office)		15. SECURITY CLASS. (of this report) Unclassified
		15a. DECLASSIFICATION/DOWNGRADING SCHEDULE

16. DISTRIBUTION STATEMENT (of this Report)

Approved for public release; distribution unlimited.

17. DISTRIBUTION STATEMENT (of the abstract entered in Block 20, if different from Report)

18. SUPPLEMENTARY NOTES

19. KEY WORDS (Continue on reverse side if necessary and identify by block number)

Aluminum Alloys	Microstructure
Aluminum Powder Metallurgy	Mechanical Properties
Processing	
De-gassing	
Oxide skin	

20. ABSTRACT (Continue on reverse side if necessary and identify by block number)

The present investigation is the first phase of a comprehensive in-house program within the Structural Metals Branch of the Materials Laboratory to study the oxide skin on aluminum powder particles. This phase is concerned with identifying the oxide and determining how the oxide is distributed during processing. Later phases will be directed towards relating the oxide skin distribution to mechanical properties.

(20. Abstract Continued)

The oxide skin has been observed at various steps of powder metallurgical processing of aluminum alloys including atomization, consolidation (compaction and degassing), forging, and extrusion.

As-atomized powder particles have an oxide skin which appears amorphous in the TEM with a thickness of typically 50Å. Occasionally nucleation of crystalline oxide has been observed (γ-Al_2O_3, MgO). In hot pressed compacts, the oxide skin is partly separated from the particle surface but still located between particles. Forging distributes the oxide skin into the original powder particles, following the matrix flow in deformation.

To follow the oxide in extrusion, mixtures of different alloy powders have been processed. In this deformation mode, the oxide skin is mainly broken-up by the shear component, but not moved significantly away from the original particle surface in the transverse direction. Distribution and shape of oxides varies from coarse to fine and rounded to irregular, depending on the process parameters.

The first step of the oxide break-up mechanism appears to be the separation of the oxide skin from the powder surface to which it is only weakly bonded. The second step is the distribution of the film fragments during deformation which depends on the mechanical properties of the oxide skin. Initially, the oxide skin on as-atomized powders behaves in a ductile manner. The oxide film, however, appears to be embrittled by degassing or heat treatment, facilitating break-up into fine fragments.

AFWAL-TR-4157

ACKNOWLEDGMENTS

F. H. Froes, W. M. Griffith, and Y-W. Kim contributed a substantial portion to this report by discussing the experimental results and offering valuable comments and suggestions for explanation of the observed effects. I also would like to thank these colleagues for reading and correcting the manuscript, and ensuring that the final manuscript was issued in my absence.

I acknowledge the contribution of people at AFWAL and DFVLR involved in the experimental and analytical work.

During this program, I had the chance to discuss the oxide problem with people at various U.S. research laboratories. I gratefully acknowledge this input. In particular, I want to thank J. P. Celis for his contribution to the development of the electrolytical embedding of powder particles, H. J. Dudek for performing AES-analyses, G. Franti for UTW-EDA of oxides in extrusions and F. Billman for supplying Li-alloyed Al powder products.

Accession For	
NTIS GRA&I	V
DTIC TAB	☐
Unannounced	☐
Justification	
By	
Distribution/	
Availability Codes	
Dist	Avail and/or Special
A-1	

iii

AFWAL-TR-83-4157

TABLE OF CONTENTS

LIST OF ILLUSTRATIONS

LIST OF ILLUSTRATIONS (Concluded)

SECTION I

INTRODUCTION

Powder metallurgical processing of aluminum alloys is complicated
because of the oxide skin that forms on the surface of powder particles.
Sintering of aluminum alloy powders in the solid state does not produce
the desired mechanical properties in these alloys since the oxide film
has to be modified to a certain extent in order to achieve bonding
between particles (Reference 1). This is obtained by deforming the
particles sufficiently to allow them to be "welded" to each other. The
remnants of the original oxide film are broken-up and distributed in the
final product, e.g., by forging or extrusion. This process is not
understood in detail, nor is the effect on the mechanical properties of
the product. It is known that degassing of powder or green compacts is
a critical processing step related closely to the oxide skin
(Reference 2). However, deformation conditions in forgings and
extrusions are equally important. To identify parameters affecting the
mechanical properties and related to the oxide distribution, the
following approach has been proposed.

a. Identify the oxide in powder and product.

b. Define the oxide distribution in powder and product.

c. Determine the relation of oxide distribution to mechanical
properties in PM products.

This work is concerned only with the oxide identification and distri-
bution. The second part relationship of the oxide distribution to
mechanical properties is being addressed in a parallel program within
the Structural Metals Branch, AFWAL, Materials Laboratory.

Because of the very fine distribution of oxide observed in certain
processing conditions, there has been some confusion in the past
regarding oxide identification. In the present investigation, several

1

microscopical and analytical methods have been applied to follow and
identify the oxides. These were performed starting with a coarse
distribution of oxide and progressed to a condition in which there were
very finely distributed oxides. The oxide distribution observed may be
modified depending on composition and structure of oxides, atomization
method, degassing practices and processing conditions. Essentially, the
oxide skin was followed through the P/M processing steps and related to
processing parameters.

Next to the oxide distribution, the mechanism of "breaking-up" the
oxide skin is of particular interest. It is expected that a better
understanding of this process may help optimizing conditions favoring a
fine oxide distribution.

The role of the oxide skin has been pointed out in a number of
publications on powder metallurgy of aluminum alloys. Sintered aluminum
powder (SAP) probably was the first material where the oxide played an
important role (References 3, 4 and 5). Emerging mechanically-alloyed
powders are produced by mechanically distributing oxides (References 6
and 7). In other high strength aluminum alloy powders, the oxide skin is
present as a consequence of the air-atomization process and not
intentional.

Effects of oxide inclusions have been reported on grain growth, re-
crystallization behavior and stabilization of microstructure. With
respect to mechanical properties, a dispersion hardening effect has been
considered as a contribution to the strength of the material. On the
other hand, oxide inclusions may have an adverse effect producing a
stress concentration and acting as initiation sites for fatigue cracks
(Reference 8).

For the discussion of these effects, any information on the oxide
distribution is valuable. A fine homogeneous distribution would give
support to a dispersion hardening effect, whereas a coarse distribution,
e.g., at grain boundaries, may favor early crack initiation.

In the following, the term "oxide" refers to the oxidation product forming the oxide skin on the surface of powder particles regardless of composition and structure of this film.

SECTION II

MATERIAL AND EXPERIMENTAL PROCEDURE

In this investigation, powders of pure Al (Al99), 2000 and 7000 series and of an Al-Li-base alloy were processed and examined. Materials and processing procedures are listed in Table 1. Mixtures of powders were also produced and processed in experiments designed specifically to follow the oxide skin.

The following parameters were considered:

Atomization Method - By different powder producers, mostly air atomization, 7175 also He-atomized, Al-Cu-Mg-Li-Zr alloy flue-gas atomized.

Powder Particle Shape and/or Size Distribution - APD 16-100 μm.

Oxide Content - Via atomization method and/or particle shape, 7175 + 0.2% oxide and +0.4% oxide.

Degassing Procedure - Recommended degassing, no degassing, intentional Oxidation.

Extrusion Ratio - 1:1 to 40:1.

Deformation Temperature - Room temperature to $450^{o}C/840^{o}F$.

Heat Treatment - Preheat, solution heat treatment, aging.

Alloy Composition - By mixing of alloy particles.

Powders and products were examined by optical microscopy (OM), scanning electron microscopy (SEM), transmission electron microscopy (TEM) and scanning transmission electron miscroscopy (STEM). Analyses were performed by energy dispersive analysis (EDA) in the SEM

TABLE 1

MATERIALS AND PROCESSING PROCEDURES

Material	APD[a] μm	Degas.	Hot-Press Temp °C (°F)	Processing and Shape	Deformation Temperature °C (°F)	Ratio	Performed at
Al99	16	No	482 (900)	extrusion round bar	93 (200)	14:1	AFWAL
2124	60	Yes	480 (896)	extrusion u-shape	450 (842)	20:1	DFVLR
7175+.2ox	60	Yes	460 (860)	extrusion u-shape	430 (806)	20:1	DFVLR
7175+.4ox	60	No	460 (860)	extrusion u-shape	430 (806)	20:1	DFVLR
7091	16	Yes	482 (900)	forging	400 (752)	67%	AFWAL
7091	16	Yes	398 (750)	extrusion round bar	398 (750)	40:1	AFWAL
7175+.2ox +Al99	60 60	No	---	HERF[b] extr., round bar	300 (572)	8:1	DFVLR
7175+.2ox +2124	100 100	No	470 (878)	extrusion rect. bar	440 (824)	24:1	DFVLR
7175+.2ox +2124	60 60	No	---	extrusion round bar	204 (400)	7:1	AFWAL
7175+.2ox +2124	30 30	No	---	HERF round bar	400 (752)	7:1	DFVLR
7175+.4ox +2124	100 100	No	470 (878)	extrusion rect. bar	440 (824)	24:1	DFVLR
7175+.4ox +2124	30 30	No	---	HERF round bar	400 (752)	7:1	DFVLR
7091 +Al99	16 16	No	---	extrusion round bar	93 (200)	14:1	AFWAL
Al-Cu-Mg-Li-Zr	NA[c]	Yes	NA	rolling plate	NA	67%	Alcoa

[a]APD = Average Particle Diameter.

[b]HERF = High Energy Rate Forming.

[c]NA = Not Available.

TABLE 2

CONDITIONS EVALUATED AND OBSERVATION METHODS

Alloy	A199	2124	7175	7091	7175 +A199	7175 +2124	7091 +A199	Al-Li Base
Producer	Eckart Reynolds Alcoa	Eckart	Eckart	Alcoa	Eckart Eckart	Eckart Eckart	Alcoa Reynolds	Alcoa
APD[a], μm	60 16 15	60	60	16	60/60	100/100 60/60 30/30	16/15	
Powders								
LM	b	b	b	b				--
SEM	b	b	b	b		See components		--
TEM	b	c	c	c		of mixtures		--
TEM-DIFF	b	d	c	c				
AES	--	--	d	--				--
Degassing procedure	No	Yes	Yes (various)	Yes	No	No	No	Yes
Hot-Pressed								
TEM	c	b	b	c	c	c	--	--
TEM-DIFF	d	d	d	d	d	d	--	--
Forged								
TEM	--	--	--	c	--	--	--	--
Extruded								
LM	c	b	b	b	c	c	c	--
SEM	c	b	b	b	c	c	c	--
SEM/EDA	--	--	--	--	c	c	c	--
TEM	c	c	c	c	c	c	c	c
TEM-DIFF	AC[d]	AC[d]	A[d]	A[d]	A[d]	A[d]	A[d]	A[d]
STEM-EDA	--	--	--	c	c	UTW[d]	c	--

---

[a] APD = Average Particle Diameter.

[b] Earlier investigation (DFVLR).

[c] This investigation.

[d] Result on oxide structure or composition, A = amorphous, C = crystalline.

and STEM, ultra-thin-window (UTW-) EDA in the STEM and by Auger-electron spectroscopy (AES). Conditions examined and observation methods used are listed in Table 2. The individual examination methods were used to develop the information listed in Table 3.

TABLE 3

EXAMINATION TECHNIQUES

OM:	Dendritic structure of powder particles, particle shape after compaction, grain morphology in compacts.
SEM:	Powder particle shape and surface topography.
TEM:	Imaging of oxides at high magnification (max. 200,000x), determination of oxide distribution.
TEM/DIFF:	Diffraction patterns (spot or ring) from crystalline oxide, diffuse patterns from amorphous film.
EDA-SEM:	Element analysis for identification of alloy particles, composition, element distribution.
EDA-STEM:	Composition analysis for powders, precipitates, and second phases.
UTW-EDA-STEM:	In addition to EDA detection of oxygen (approximately 80%) and carbon (approximately 20%) x-ray-radiation.
AES:	Composition of surface layers on powder particles, depth composition profile by sputtering, detection of O, C, Mg, Al.

Information on various techniques of surface analyses is given in References 10, 11, and 12. In this investigation, only AES has been used for surface analysis. For TEM in this program, a special method was developed for preparing sections of small powder particles (References 13 and 14). In this method, particles are electrolytically embedded in a nickel foil (Figure 1). TEM specimens were prepared by

jet-polishing the foil in a mixture of 20% HNO_3 and methanol at -45°C (-50°F). Since this process may have an effect on the oxide, at least one sample was prepared for comparison by ion-milling for every condition whenever information on the oxide skin was obtained. Oxidation during ion-milling is restricted to "natural" oxide skin and is not assumed to cause any change in the oxide distribution investigated.

SECTION III

RESULTS AND DISCUSSION

1. POWDERS (A199, 2124, 7175, 7091)

Most of the information on the oxide skin was obtained by TEM. A typical nickel-foil with alloy particles is shown in Figure 2. Although the resolution in this image is not high enough to reveal any details in the oxide skin, it can be seen that the oxide film is not removed completely from all particle surfaces by the ion-milling process. The dendritic structure of the particle is revealed by the etching effect of ion-milling. At higher magnification, the dendritic particle surface embedded in nickel can be seen, Figure 3 (arrow). The oxide skin observed on as-atomized powder is very thin and makes imaging of the surface film perpendicular to the foil surface difficult. Once the skin has been removed from the surface, imaging and production of diffraction pattern is less difficult, as will be shown later. Because of the imaging conditions, the exact thickness of the oxide skin could not be determined. However, from all instances where the oxide skin was imaged, it could be concluded that its thickness does not exceed 50$\overset{\circ}{A}$.

In the 2124 alloy powder investigated, the oxide skin has been partly removed during ion-milling or could be imaged very close to the TEM-foil edges (Figure 4). Diffraction patterns indicate that the oxide film is amorphous, since only a diffuse halo was observed with no evidence of discrete spots or rings (Figure 5). However, in a few locations, very small prticles in the oxide film could be imaged in bright and dark field conditions (Figures 4 and 6). The particle size was in the range of 10 to 50$\overset{\circ}{A}$ and sharp diffraction rings were obtained. Evaluation of the diffraction pattern indicated that the observed phase was MgO (Table 4). Frequently, oxide skin has been found in inter-dendritic regions close to the particle surface (Figure 7). These regions are close to locations, where crevices between dendrites on the particle surface terminate (Figures 8 and 9). These oxides may not be affected by degassing as effectively as is the surface oxide skin.

9

TABLE 4

DIFFRACTION PATTERN ANALYSIS IN 2124 POWDER

Diffraction Pattern L = 41$\overset{\circ}{A}$ mm^{-1} MgO (ASTM)

Ring Radius R, mm	Relative Intensity	d-spacing $\overset{\circ}{A}$	d-spacing $\overset{\circ}{A}$	Relative Intensity	hKl
17	5	2.41	2.431	1	111
19.5	10	2.10	2.106	10	200
27.5	7	1.49	1.489	5.2	220
			1.270	0.4	311
32.5	<1	1.26	1.216	1.2	222
34.5	1	1.19 ?			
40	<1	1.025	1.053	0.5	400
			0.967	0.2	331
44.5	1	0.92	0.942	1.7	420
49	<1	0.84	0.860	1.5	422
			0.811	0.3	511

AES was performed on a few selected specimens of air-and helium-atomized 7175 powder. The distribution of elements determined after sputtering of the particle surface is shown in Figure 10. The oxide skin in this alloy contains Mg, Al, and O. The air-atomized powder shows a higher degree of oxidation. From these data and the corresponding sputtering rate for a Ta_2O_5 standard (330Å/min), the oxide skin thickness can be estimated. Assuming that the sputtering depth at half maximum of the oxygen-signal indicates the oxide skin thickness, 130Å, is obtained for air-atomized powder and 185Å for He-atomized powder. This result is somewhat surprising because a thinner oxide skin would be expected with He-atomization. Furthermore, the oxide thickness determined by AES is not in agreement with the thickness determined by TEM in this investigation (typically 50Å). Different methods of thickness determination of the oxide skin on aluminum alloy particles, e.g., by SIMS, ISS and NMR (References 17, 18 and 19) support the thickness of 50Å range rather than above 100Å. In general, the geometry effect is an important factor in thickness determination of surface layers with AES. Sputtering through a flat, well-defined surface would give a result close to the actual thickness measured from the change in signal intensity. In a rough surface the signal from unremoved oxides would change not only the steepness of the gradient but also the absolute reading of the measured oxygen. This is especially true for sputtering of loose powders. The geometry effect would cause an over-estimation of the oxide thickness. These effects and the applicability of AES for thickness measurements have been observed and discussed (Reference 15).

2. COLD- AND HOT-PRESSED POWDERS (A199, 7175, 7091 AND MIXTURES)

The TEM-image of hot pressed powders shows in many cases the double oxide skin (~50Å) between two powder particles (Figure 11). The film is occasionally separated from the particle surface, especially at higher pressing temperatures. Due to the small amount of deformation, very little break-up of the skin has been observed.

11

The oxide film shows its typical contrast in TEM, when removed from the surface. A very fine-grained structure, powdered contrast which changes little with tilting angle, indicates an amorphous or micro-crystalline structure.

For identification of the oxide film, A199 powder was intentionally oxidized and compacted at $480^{\circ}C$ ($900^{\circ}F$) for 1 hour (Figure 12). This oxide film showed the same contrast as the oxide skin observed in the other alloys investigated. Electron beam diffraction showed patterns indicative of amorphous material with a certain amount of γ- (or η-) Al_2O_3 for the A199 compacts (Figure 13 and Table 5). The system of very fine diffraction rings indicates that the crystallite size of Al_2O_3 nucleated in the oxide skin is extremely small, (probably ~10Å). This is in accordance with the limited thickness of the film of approximately 50Å determined by the major number of TEM observations. γ-Al_2O_3 is the phase which might be expected to be formed on pure aluminum during atomization (high temperature/high cooling rate). Nucleation of γ-Al_2O_3 in the amorphous film may also occur during hot-pressing, especially with oxygen present (References 20, 21 and 22).

TABLE 5

DIFFRACTION PATTERN ANALYSIS FOR A199 COMPACTS

Diffraction Pattern $\lambda L=25$Åmm^{-1}			γ-Al_2O_3 (ASTM)		
Ring Radius R, mm	Relative Intensity	d-spacing Å	d-spacing Å	Relative Intensity	hKL
			4.56	4	111
			2.80	2	220
			2.39	8	311
10.7	2	2.34	2.28	5	222
12.7	9	1.97	1.997	10	400
			1.520	3	511
17.7	10	1.41	1.395	10	440
22	1	1.14	1.140	2	444
			1.027	1	731
			0.989	1	800
			0.884	1	840
			0.806	2	844

Electron beam diffraction analyses of alloy material throughout all processing steps in this investigation indicate that the thin film observed is amorphous of microcrystalline, as is the film identified in A199. In addition, UTW-EDA has been applied to verify that the observed film in extruded alloy material contains oxygen and is the oxidation product in question (Figure 14). All oxide skin fragments observed seem to have a rather uniform thickness.

In some cases, very small MgO crystals have been observed in the oxide skin residues in extrusion, e.g., in 2124 alloys. These alloys already showed MgO crystals in the oxide skin of the powder. This may explain why MgO was also observed in extrusion, however, crystallization of MgO may also have occurred during high temperature extrusion. In some instances, crystallization of MgO in the amorphous oxide skin could be caused by heating the specimens locally with the electron beam.

During hot-pressing, recrystallization may occur if deformation and temperature are high enough. In many cases, the double oxide skin does not appear to prevent grain growth from one particle to the next through their surfaces, even between powder particles of different alloy compositions. The oxide skin also does not seem to hinder diffusion of alloying elements at solution heat treatment temperatures of different alloys. This has been reported for cold-rolled material processed from a mixture of two different alloy powders (Reference 23). Because of the oxide skin, it is generally possible to locate the original powder surface even after recrystallization of hot-pressings. However, this is extremely difficult in material processed to high extrusion ratios (higher than 5:1 in round-bar extrusions), because of severe deformations and recrystallized grains present.

TEM of hot-pressed powders shows that the oxide skin may be removed from the powder particle surface even at smaller amounts of deformation. The oxide film appears to prevent bonding between particles in this step of processing. Although different degassing procedures have been used in this study, the effect of degassing on the oxide skin prior to

hot-pressing has not been investigated. However, this appears to be of great importance for the understanding of some of the following findings and should be studied in detail.

3. FORGINGS AND EXTRUSIONS[a]

The oxide skin present in hot-pressed material is probably completely separated from the original particle surfaces in the forging process, in the form of stringers or flakes (Figure 15).

Forgings from an earlier program (Reference 24) were examined in the TEM. The particles forming the stringers unfortunately were too small to be analyzed or identified as oxides. For this reason, an indirect method was developed which evaluates the material flow during deformation and can be applied to indicate the path of the oxide away from the original particle surface during processing. For experimental reasons, this method was applied to extruded material and will be described below.

Unlike forgings, all extrusions produced after properly degassing showed finely dispersed oxide skin residues (2124, 7175, 7091). These extrusions were generally produced at higher ratios (20:1, 20:1, 40:1, respectively), which favors the break-up of the oxide skin. The 7091 material showed the largest dispersoids, most likely because of the relatively fine average particle diameters (APD) of 16μm of the powder processed compared to 60μm APD in the other alloys (Figures 16 and 17).

As observed in TEM, these particles were inhomogeneously distributed, sometimes in stringers, and were too small to be analyzed. However, the fine particles were insoluble by solid solution treatments and their image contrast was identical to the oxide skin previously observed. Thus, it has been assumed that these are fragments of the

---

[a]All material in Table 2.

oxide skin. To validate this assumption, the process of the oxide
break-up has been studied in detail by two different experiments:

a. The amount of oxides has been increased and the rate of
breaking-up decreased so that the oxide could be followed easily, and

b. A method of marking the original powder particle after
deformation has been developed so that the small particles could be
associated with the particle surface. This method allows indirect
identification of oxide skin residues and the material flow and the
mechanism of breaking-up of the skin by extrusion.

Hot-pressed A199, artificially oxidized, has been extruded 14:1 at
$93^{o}C$ ($200^{o}F$). Figure 18 shows the extruded microstructure. The oxide
film has been separated from the original particle surfaces, but is still
predominantly present between particles or has been incorporated into
the soft aluminum. It essentially prevents bonding between the metal
particles. Obviously, this is an example for extremely unfavorable
conditions for producing powder products. The film fragments are large
enough to be identified in the extrusions by the methods described
previously with the hot-pressed products.

The large flakes of oxide skin suggests that the oxide skin in this
condition is rather ductile or flexible. The microstructure of the A199
extrusion resembles that of extrusions of mixtures of aluminum powders
with some soft polymer fibers or powders (e.g., polyethylene-terephtalate
(Reference 25)). In both cases, the oxide film and the deformed polymer
may prevent bonding between the aluminum powder particles.

Extrusions of heavily oxidized aluminum showed that in the extruded
structure, the oxide skin is found mostly at the powder particle
interphases. Only a small fraction of oxides is found inside the soft
aluminum particles. At higher extrusion ratios, this process is assumed
to be essentially the same except that with the higher elongation of the

particles, the spacing between oxide stringers decreases. In addition, oxide skin fragments located at the powder surface are increasingly torn apart from each other with higher extrusion ratios.

If the fine particles observed are assumed to be oxide skin fragments, more information of their origin would be obtained. Unfortunately, the powder surfaces are difficult, if not impossible, to locate in high ratio extrusions, as discussed earlier. To overcome this problem, mixtures of 50:50 wt. percent powders of different alloys have been extruded. In this way each powder could be identified in the TEM.

The first approach was a mixture of 50% Al99 and 50% 7091, extruded 14:1, where the alloy is easy to recognize in the SEM because of the contrast due to the difference in composition (Figure 19). In the TEM, 7091 was clearly recognized because it contains Co_2Al_9 dispersoids. Because of the relatively coarse distribution, however, Co_2Al_9 does not delineate the boundaries accurately. An aging treatment was given to form fine precipitates in 7091 powders, so that the boundaries between both materials were revealed (Figure 20). A similar experiment was performed with a mixture of 7175 and Al99 extruded 8:1. The result of these experiments showed that the degree of oxide skin break-up increases with extrusion ratio. Particles assumed to be fractions of the oxide film indeed were associated with original particle surfaces or at least found very close to these surfaces. In the following examples, the material flow following extrusion and the concurrent motion and breakup of the oxide skin are described.

The dark region around the 7091 particle in Figure 21 shows a large amount of oxide skin because of the low amount of deformation, whereas the skin is much more broken-up in the elongated tail-section of this particle (Figure 22). The oxide film may be found closely attached to the particle (but probably not strongly) or piled up against the 7175 powder particle in the softer Al99 powder (Figure 23). Figure 24 shows grain growth through the particle surface even at this low deformation temperature (93°C, 200°F). In a regular extrusion, the particle surface probably would have been undetectable. The break-up seems to be directly

16

related to the orientation of the skin relative to the extrusion
direction or the amount of shear deformation. Figure 25 shows the
difference in oxide skin motion parallel to the extrusion direction and
perpendicular to the extrusion direction. Generally, the oxide film is
torn apart in extrusion direction, but moved very little in the
transverse direction or away from longitudinal particle boundaries.

The mixture of 7091/A199 represents hard particles in a soft matrix
and the material flow must be expected to be different from extrusions
of like powders. Additional experiments were carried-out with two alloy
powders of approximately equal strength, a mixture of 50% 2124 and 50%
7175. The SEM examination shows similar deformation behavior between the
two alloy powders in the 2124/7175 mixture, in contrast to the Al7091
mixture in which a larger difference was observed (Figure 26). However,
the break-up of the oxide skin and the material flow in extrusion are
very similar to each other and confirm the description of the
distribution process described previously. The amount of oxide observed
was much less in the mixture extruded at 440°C (825°F) compared to the
205°C (400°F) extrusion. However, diffusion that occurs during the 400°C
extrusion made the two different alloy powders indistinguishable.

Additional experiments with extrusions of HERF powder mixtures did
not add information to the understanding of the break-up process. The
result on the oxide distribution in these experiments were essentially
the same. All oxides observed stem from oxide skin fragments and were
all distributed inhomogeneously in the extrusion direction.

Skin fragments were observed from extremely small and finely
distributed to intermediate flakes with irregular shaped or rounded
edges. The largest fragments occurring were tangled or folded and seem
to consist of plastically behaving oxide skin.

Three typical oxide distributions observed are summarized as follows:

a. Large tangled residues of oxide skin (on the order of 1μm), coarsely distributed, high volume content. Observed in intentionally oxidized A199 extrusion and Li-containing Al alloys. Generally, a detrimental effect on mechanical properties can be expected (Figures 18, 28 and 29).

b. Intermediate or rather large film flakes, rarely folded or tangled (on the order of 1000Å), small to high volume fraction. Observed generally with low temperature extrusion; without degassing procedure; reduced mechanical property levels expected (Figure 27).

c. Very small residues (~30Å) at the detectability limit of TEM bright field image, inhomogeneously distributed, very small volume fraction. Typical for material with good mechanical properties produced by accepted procedures (Figure 17).

Larger residues of oxide skin often appear to behave like a plastic or elastic film. They are folded or tangled into a three-dimensional arrangement. If this happens to a more brittle film, it would break at the folded edges. In this way, the ductile or brittle nature of an oxide skin is determined from the shape it appears in after deformation.

During electrolytical jet polishing or ion-milling, the metal around the oxides is removed. For both thinning methods, the oxide skin is not removed at the same rate as the metal, especially in the case of ductile film. Thus in TEM, film flakes are partly located at the surface of the thin foil. However, TEM observations indicate that film residues are also located inside the sample material.

Large oxide residues were identified by their contrast in TEM bright field image and by their location relative to the original particle boundaries. Electron beam diffraction showed patterns indicating an amorphous structure of the film. This may be due to the fact that

18

most extrusions were produced at low temperatures and without degassing. At higher temperatures, there is a possibility of crystalline oxide nucleation during hot-pressing or during degassing, as observed with MgO in 2124.

Intermediate size oxide particles were analyzed by UTW-EDA in the STEM as reported earlier in this section.

Generally, the shape of the oxide film flakes varies with the physical properties of the oxides and processing conditions. Film edges are serrated and irregular or well-defined and rounded. In some cases, a coagulation of oxide skin residues has been observed. Those features varied with the time period after sample preparation and storage in the desiccator. However, it is not clear whether only oxide film portions on the TEM-foil surface are affected or also those inside the thin foil.

The following parameters have been found to play a role in the oxide distribution in extrusions:

- degassing
- deformation temperature
- amount of shear deformation

The oxide distribution changes from coarse to fine with a more effective degassing procedure and with increasing deformation temperature and shear deformation amount. Three other parameters have been expected to have effects on the oxide distribution:

- oxide content of the powder
- particle shape
- particle size distribution

These parameters have not been varied systematically in this investigation and no evaluation of effects on oxide distribution can be reported. However, a higher density of oxide skin residues has been

observed in extrusion made from fine powders compared to coarse powders (7175/2124 - 30μm APD compared to 60μm).

The mechanism of breaking-up the oxide skin has been found to be the same in all experiments, that is, it depends only on the nature and properties of the oxide skin. It can be described in two steps, both occurring during extrusion:

a. Separation of oxide skin from particle surface

b. Distribution of broken-up film fraction:

(1) Oxide film behaves in a "brittle" manner:

Film is broken-up into small pieces with no folding of film or overlapping, finely distributed but not homogeneous; oxide residuals still concentrated in stringers close to original particle surface. This distribution should not strongly degrade mechanical behavior.

(2) Oxide film behaves in a "ductile" or "elastic" manner:

Film is folded and crumpled up, frequently overlapping; distributed in longitudinal direction, very coarse. This distribution is likely to be deterimental to mechanical behavior.

A typical example for step 2b has been observed in flue-gas-atomized Al-Li-base powders after extrusion. The oxide skin is retained in larger flakes which are removed from the powder surface during extrusion but cannot be broken because of the ductile-elastic-plastic behavior (Figures 28 and 29). These conditions resemble the extrusion of aluminum powders with certain plastics (Reference 25). In this condition, the oxide film tangles do not completely fill the cavity around them, again similar to plastics in aluminum extrusions. These voids will be detrimental to mechanical properties. Poor fatigue properties in some of the Al-Li base alloys have been attributed to oxide at the grain boundaries (Reference 26).

SECTION IV

SUMMARY

The objective of this investigation was to obtain information on the distribution of the oxides in P/M aluminum alloy products. In this study, examination has been concentrated on the oxide distribution in the final powder product: conventional or HERF[a] extrusions.

Two factors control the oxide distribution in extrusions: the matrix flow in deformation and the properties of the oxide film to be dispersed. The geometrical distribution is determined mainly by the plastic flow in the metal whereas size and shape of the oxides are strongly affected by the mechanical properties of the oxide skin.

1. DISTRIBUTION OF OXIDE RESIDUES

Following the matrix flow in extrusion, oxide skin fragments located at or near particle boundaries are moved apart from each other in the longitudinal direction. With higher extrusion ratios, these stringers or flake arrangements get closer to each other in the transverse direction and the dispersion of oxide skin residues is more uniform than at low extrusion ratios. However, this distribution is far from being homogeneous. The distribution achieved depends also on the particle size after break-up.

The bond between the oxide skin and metal is apparently not very strong and the break-up occurs in the early stages of the deformation process. After the skin has been removed from the surface, it is still located close to it, but dispersed in the extrusion direction. A similar effect is expected in forgings.

[a]High Energy Rate Forming.

2. BREAK-UP OF OXIDE SKIN FRAGMENTS

The break-up process has been found to be strongly affected by the mechanical or physical properties of the oxide skin. Plastic/elastic skin is very difficult to break-up, but brittle oxide skin will be broken into small pieces or particles relatively easily.

Oxide skin properties appear to be significantly affected by degassing procedures. Deformation temperature plays an equally important role. It is not clear whether oxide film properties are changed with deformation temperature or deformation amount.

SECTION V

CONCLUSIONS

Oxides observed in P/M aluminum alloy products are broken-up fragments of the oxide skin from powder particles. Extrusions of properly degassed compacts show a small amount of fine oxides. This observation indicates that only minor contributions to strengthening and microstructure stabilization may be expected from the dispersion. An adverse effect on mechanical properties may be seen in the extrusions produced at low temperatures, without degassing or with Li-containing alloys. In such extrusions, the breakup of the oxide skin is incomplete and the distribution is localized. This type of oxide distribution is assumed to have a "weakening-effect" on the structure.

The main problem in aluminum powder metallurgy regarding the oxides is how to break-up the oxide skin fragments properly during processing. This will be achieved by properly controlling the following:

a. Processing conditions:

- processing temperature
- deformation mode
- deformation ratio

b. Deformation properties of oxide skin:

- alloy composition
- composition and structure of oxide skin
- degassing procedure
- deformation temperature

SECTION VI

FUTURE WORK

Similar experiments of powder mixture extrusions are suggested for forged material. For forgings, in particular, an isotropic shear deformation may be expected with special forging techniques. Parameters should be adjusted to maximize the break-up of the oxide skin.

Systemic degassing experiments are required to better understand what controls the breakup. There are a number of parameters which may cause either plasticity or brittleness of the film. In degassing, decomposition of the oxide skin occurs and the amorphous oxide may transform partly into crystalline phases. A combination of degassing experiments and electron microscopic investigations are required to show whether removal of hydroxyls favor a more brittle behavior of the skin. The determination of the hydroxyl content of the oxide will have to be carried-out by nuclear magnetic resonance experiments. This data would have to be related to mass-spectrometrical, TEM and surface analysis data.

Crystalline oxides, MgO or $\gamma\text{-}Al_2O_3$, in the amorphous film have been observed in some cases. The transformation of the oxides, if any, in the film should be investigated in detail and related to processing conditions, e.g., hot-pressing parameters. This may answer the question on how crystallization of the amorphous skin changes its properties and if this effect plays a role in the oxide break-up. In addition, the thickness of oxide skin may play a role in determining its mechanical properties to a certain degree. Although skin thickness was not observed to vary considerably, a certain variation may be achieved by different atomization methods (air vs. inert-gas atomization).

A program for two studies extending this investigation is suggested in the following section.

1. SUGGESTED PROGRAM

    a. Forging Experiment

Purpose: To compare the nature of oxide break-up and distribution in forgings with that in extrusions. Specifically, material flow and penetration of the oxide into the material will be examined, initially keeping all conditions similar to those of extrusions already examined.

Material: Mixture of 7091 and pure Al.

Preparation:

Mix
green compact:	standard method
can:	standard method
degas:	can be a variable
consolidate:	by standard methods (start with low temperature)
forge:	start with A-upset, with option to add AB, ABC, channel-die and/or spike forgings

Characterization:

    macro examination for flow
    radial cuts in pancake ("A") forging
    foils parallel to cuts, away from low flow regions

    b. Degassing Experiment

Purpose: To determine how the precompaction environment affects the nature (morphology, distribution, etc.) of the oxide skin that may, in turn, control the properties of the final product.

    Phase I: What degassing schemes change oxide nature the most.

    Phase II: How the difference in oxide nature affects selected mechanical properties?

25

Material: Alloy (to be determined)

        Loose powders and green compacts

Degassing Variables:

        Vacuum level   high - best effort
                                    middle
                                    low - 1 atm

        Gas - inert, air, humidity (can add later)
        Temperature - based on available data on degassing
        Transfer - temperature, time, cooling rate, environment
          consolidation.

Figure 1. Cross Section of an Electrolytically Deposited Ni-Foil
Containing Aluminum Alloy Powder Particles (SEM)
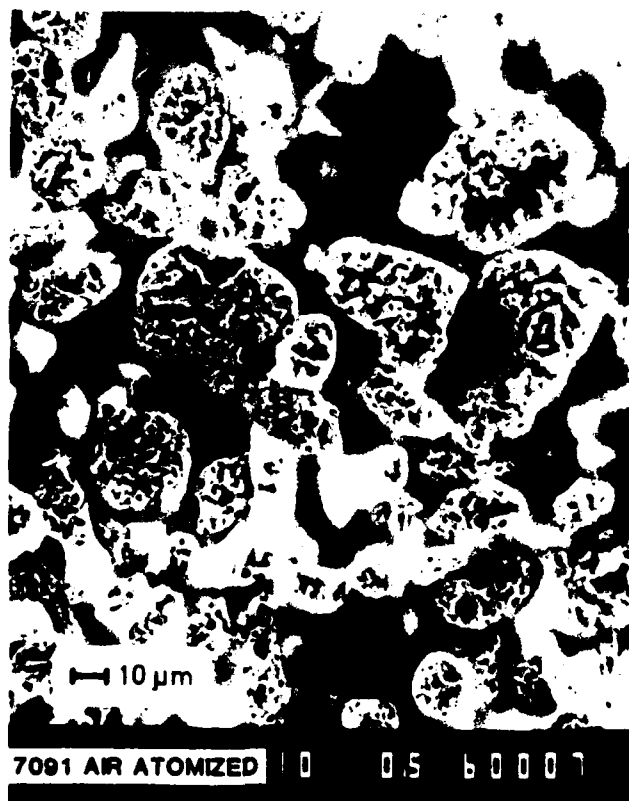
Figure 2. Thin Foil Prepared as in Figure 1 and Ion-Milled for TEM
(SEM-Mode of STEM)

Figure 3. Dendritic Structure at the Surface of a 7091-Powder Particle.
Arrow Indicates Oxide-Skin (TEM, Ion-Milled)

Figure 4. Oxide Film on an Air-Atomized 2124 Particle with MgO-Nucleation
(TEM, Bright Field, Ion-Milled)

Figure 5. Diffraction Pattern of Oxide Skin in
Figure 4, Indexed as MgO
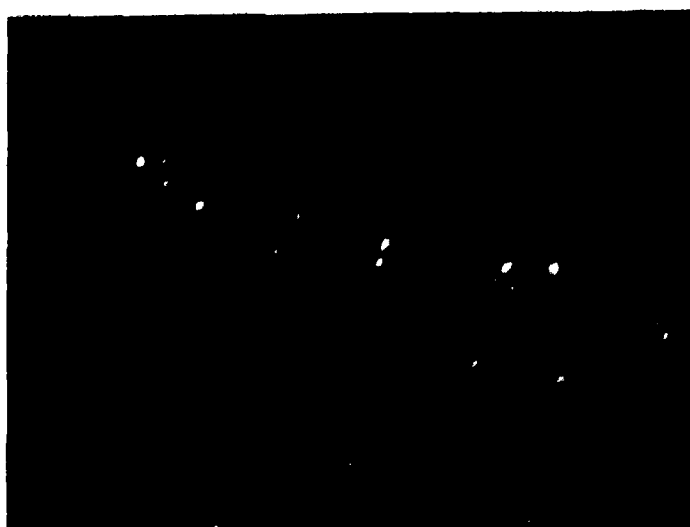
Figure 6. Dark Field Image of Region in Figure 4, Generated with
a 10° Section of the Two Inner Diffraction Rings

Figure 7. Dendritic Structure at the Surface of a 7091-Powder
Particle. Arrow Indicates Oxides in Interdendritic
Region (TEM, Ion-Milled)

7091 AIR ATOMIZED

Figure 8. Surface of 7091 Powder Particle, as Atomized (SFM)

Figure 9.   Surface of 7091 Powder Particle, as Atomized
(SEM), at Higher Magnification
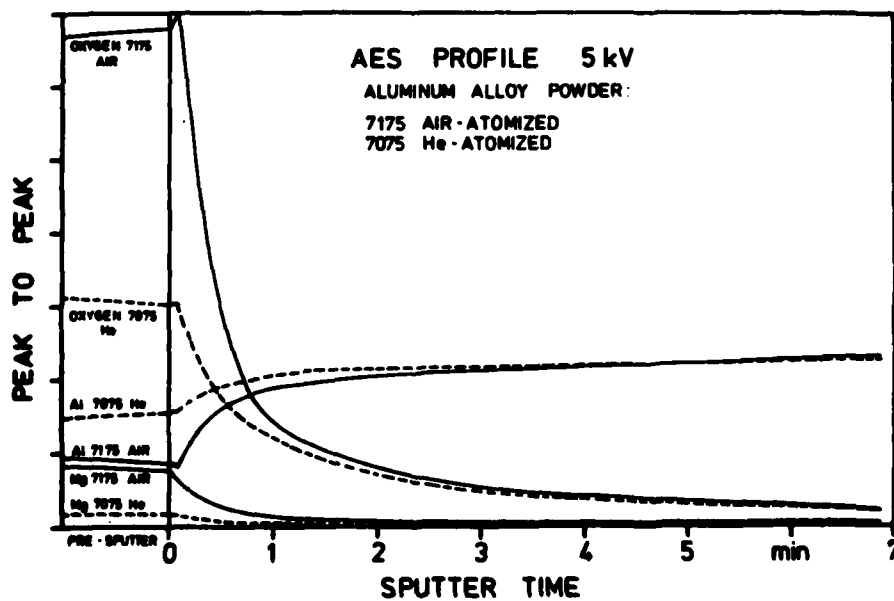
Figure 10.   Auger-Electron-Spectroscopy Depth Profile of
Helium-Atomized 7075 and Air-Atomized 7175 Alloys

31
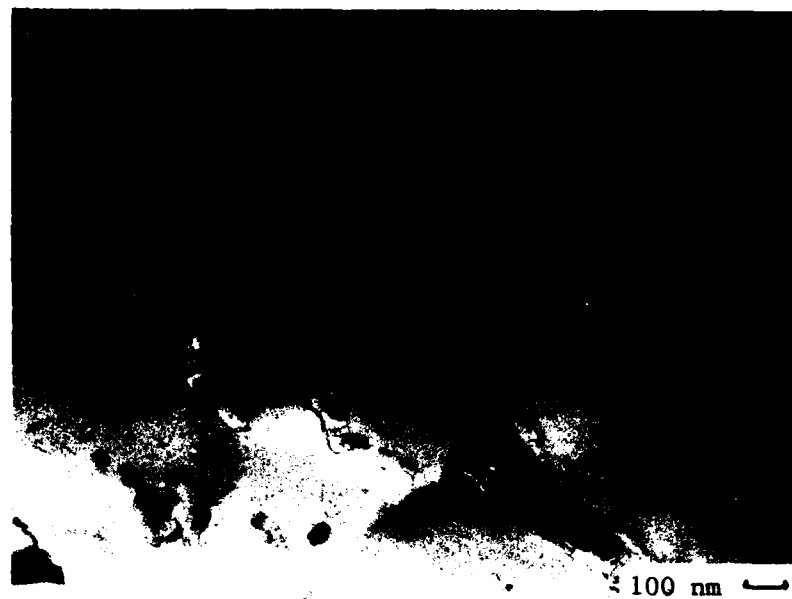
Figure 11. Double Oxide Film Between Two Hot-Pressed 7175
Alloy Powder Particles. The Interface is
Slightly Sheared (TEM, Jet-Polished)
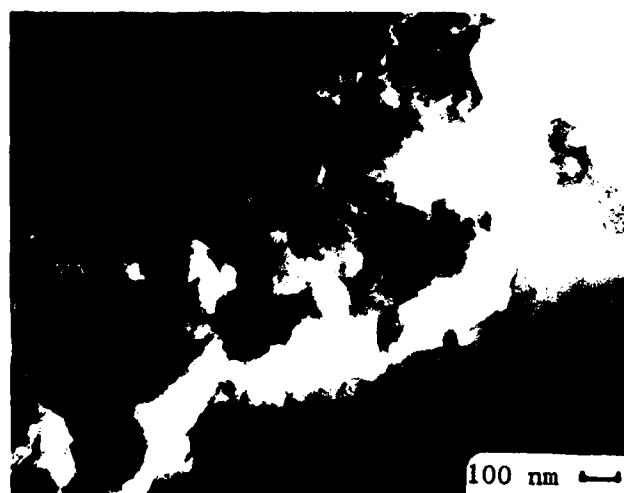
Figure 12. Commercially Pure Aluminum Powder, Intentionally
Oxidized and Hot Pressed (TEM, Ion-Milled)

32

Figure 13. Diffraction-Ring Pattern from Oxide Film
in Figure 12.
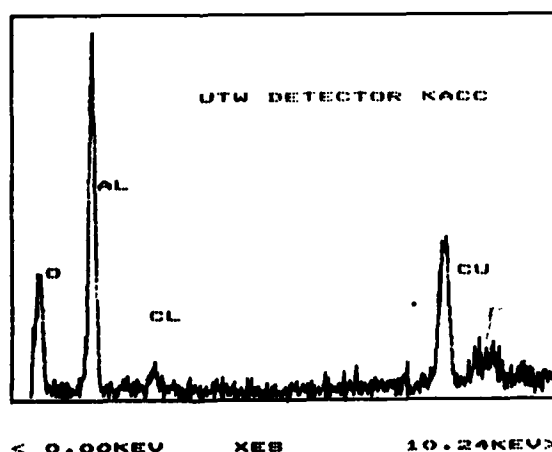
Figure 14. Ultra-Thin-Window Energy Dispersive Analysis of
Oxide-Skin Residue in the STEM. Material:
Extruded Mixture of 2124 and 7175 Alloy Powders
(Mixed 50:50)
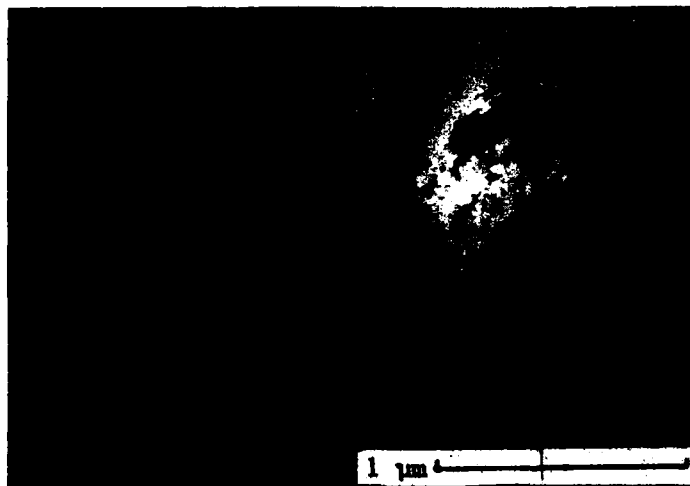
Figure 15. Oxide Stringers in a 7091 PM Forging, 67% Deformation at 400°C (752°F) (TEM, Jet-Polished)
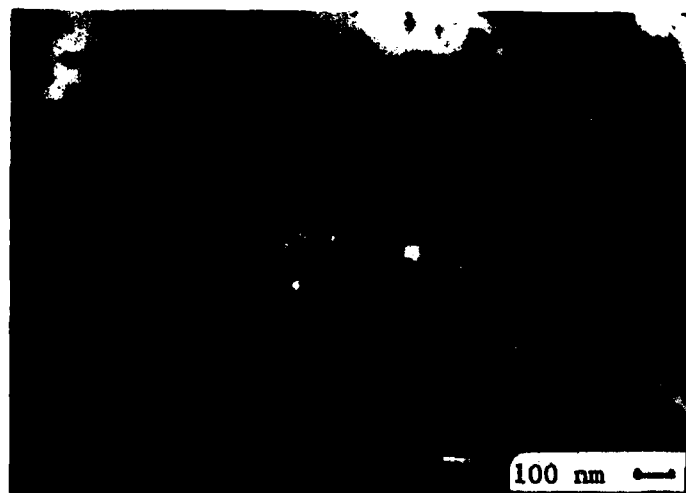
Figure 16. Oxide Stringers in a 40:1 Extrusion of 7091 PM Material, Highest Concentration Observed, Net Representative (TEM, Jet-Polished)

Figure 17. Oxides in a 20:1 Extrusion of 2124 PM Material.
Nucleation of MgO in Oxide Skin Fragments.
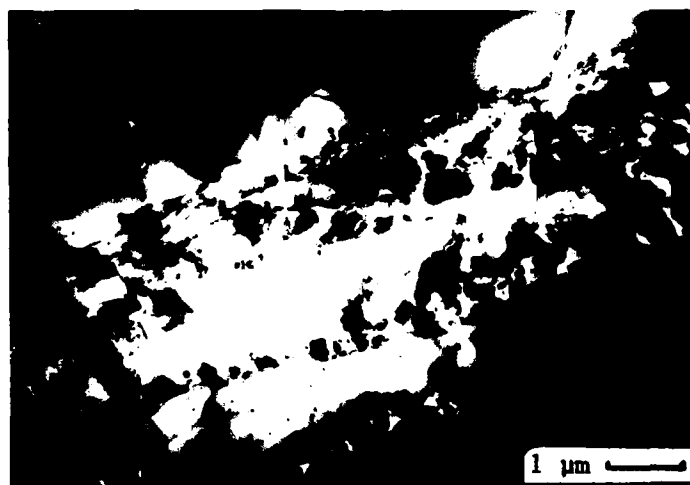Highest Concentration Observed, Not
Representative (TEM, Jet-Polished)

Figure 18. Extrusion of Intentionally Oxidized Al99
(TEM, Ion-Milled)

35

Figure 19. Extrusion of a Mixture of 7091 and AL99 (50:50, Extrusion Ratio 14:1). The Dark Phase is Al99, the Bright Phase is 7091 (SEM)
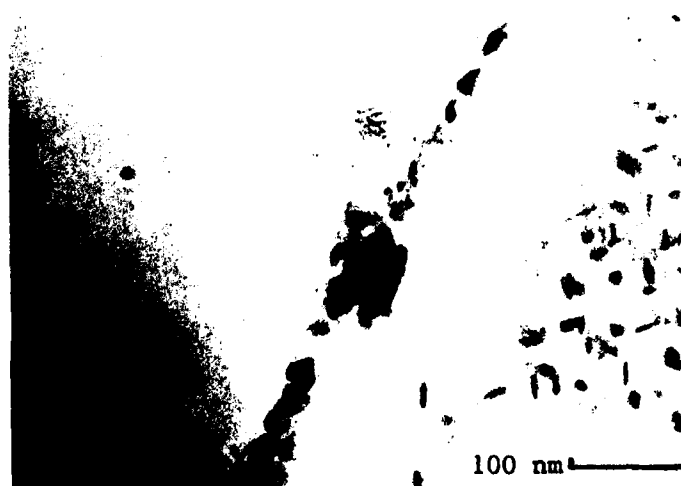

100 nm

Figure 20. Interface Between a 7091 and a Al99 Particle in the Extrusion of Figure 19 After Aging Heat Treatment (TEM, Jet-Polished)

Figure 21. Extrusion as in Figure 19 (TEM,
Jet-Polished)

Figure 22. Extrusion as in Figure 19, Region of High Shear
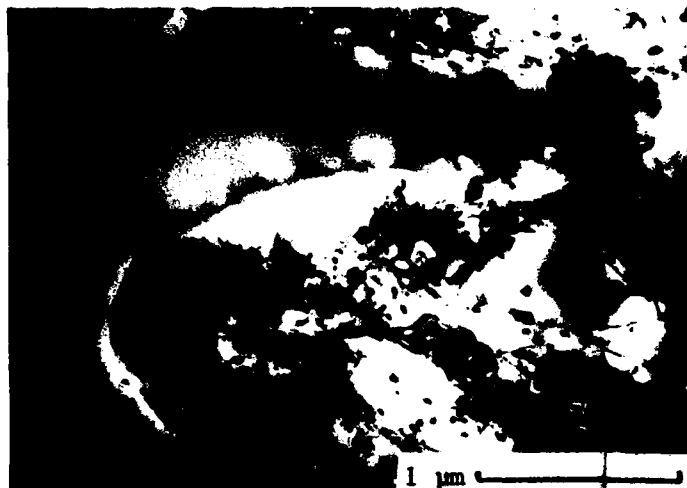Deformation and Break-Up of Oxide Skin (TEM,
Jet-Polished)

37

Figure 23. Oxide Skin Piled up in Front of a Hard 7091
Particle in a Soft Al99-Matrix (TEM,
Jet-Polished)

Figure 24. Grain Growth Through Interface Between 7091
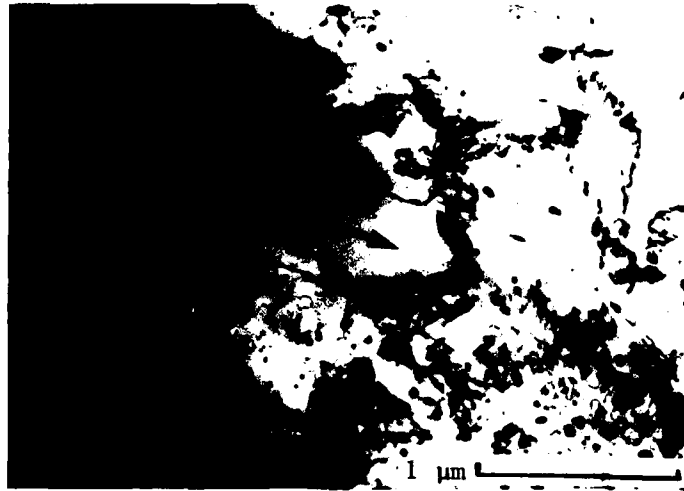and Al99. Location as in Figure 23 (TEM,
Jet-Polished)

Figure 25. Break-Up of Oxide Skin at Particle Surface
Oriented Parallel and Perpendicular to the
Direction of Extrusion (TEM, Jet-Polished)

7175/2124 EX 7:1
204°C (400°F)

Figure 26. Extrusion of a Mixture of 2124 and 7175 (50:50,
Ratio 7:1). The Dark Phase is 2124, the Bright
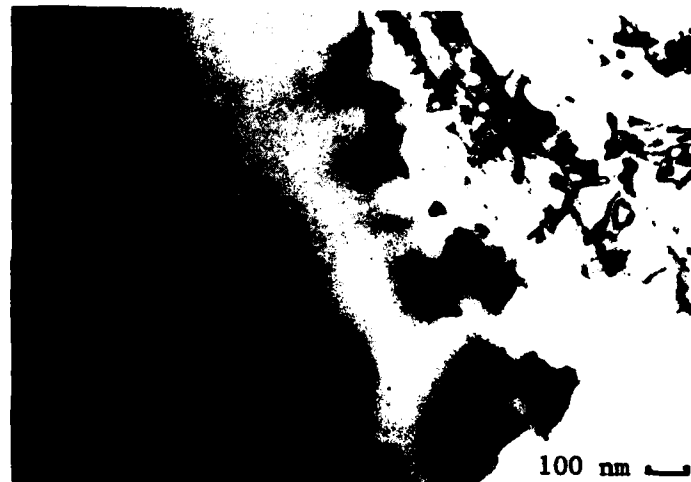Phase is 7175 (SEM)

100 nm

Figure 27. Oxide Skin Flakes in an Extrusion Produced
From a Mixture of 7091 and Al99 Powders
(TEM, Jet-Polished)

1 μm

Figure 28. Oxide Skin Residues in a Flue-Gas-Atomized
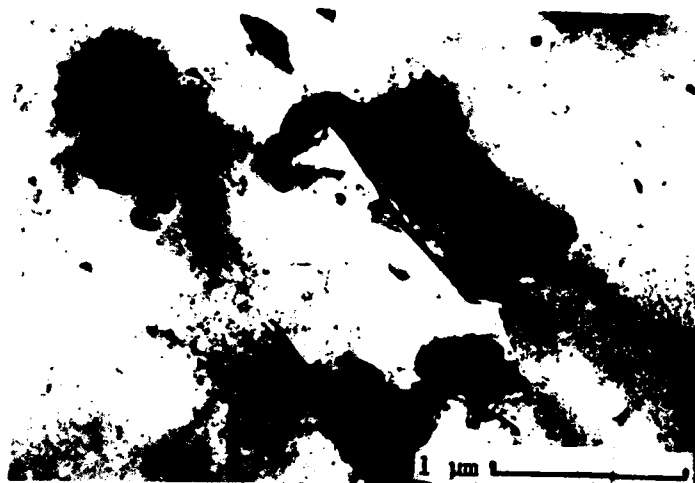AlCuMgLiZr-PM Extrusion (TEM, Jet-Polished)

Figure 29. Oxide Residues From Figure 28 at Higher
Magnification (TEM, Jet-Polished)

REFERENCES

1. F. J. Gurney, D. J. Abson, and V. Depierre, Technical Report No. AFML-TR-73-252, September 1973.

2. D. Voss, Final Report No. AFOSR 77-3440, EOARD-TR-80-1, October 1979.

3. L. F. Mondolfo, "Aluminum Alloys: Structure and Properties," London, 1976, pp. 883-893.

4. P. Guyot, Modern Developments in Powder Metallurgy, Vol. 2, 1965, pp. 112-130.

5. E. Ruedl, P. Guyot, Modern Developments in Powder Metallurgy, Vol. 2, 1965, pp. 131-144.

6. W. C. Oliver, Thesis, Stanford University, Department of Materials Science and Engineering, 1981.

7. R. F. Singer, W. C. Oliver, W. D. Nix, submitted to Met. Trans., June 1980.

8. W. C. Kuo, E. A. Starke, Jr., Met. Trans., in press.

9. H. W. Werner, Electron Microscopy, Vol. 3, 1980, pp. 200-207.

10. A. Csanady, D. Marton, and L. Kover, 7th International Light Metals Congress, Leoben/Vienna, Austria, 1981.

11. G. van der Kelen, Silicates Industriels 3, 1975, pp. 75-77.

12. W. L. Baun, T. J. Wild, and J. S. Salomon, Journal of Electrochemcial Society, Vol. 123, No. 1, January 1976, pp. 2-5.

13. G. Staniek and J. P. Celis, unpublished work.

14. S. Kirchoff, Technical Report, AFWAL, to be published.

15. K. Wefers, Aluminum, Vol. 57, No. 11, 1981, pp. 722-726.

16. M. Zayan, M. Pohl, W. G. Burchard, W. Dahl, W. Gruhl, and G. Ibe, 7th International Light Metals Congress, Leoben/Vienna, Austria, 1981.

17. K. Wefers, private communication.

18. B. R. Baker, private communication.

19. R. M. Pearson, Jornal of Catalysis, Vol. 23, No. 3, December 1971.

20. K. Wefers, G. M. Bell, Alcoa Technical Paper No. 19, 1972.

REFERENCES (Concluded)

21. H. P. Rooksby, "The X-Ray Identification and Crystal Structures of Clay Minerals," ed. G. Brown, Mineralogical Society, London, 1972.

22. M. Hansen, "Constitution of Binary Alloys," New York, 1958.

23. H. Sunwoo and D. H. Ro, TMS Fall Meeting, St. Louis, MO, 1982.

24. M. M. Cook and Y-W. Kim, Microstructural Science, Vol. 10, eds. White, Richardson, and McCall, Elsevier Science Publishing Company, 1982.

25. G. Staniek and J. Petermann, unpublished work.

26. A. Gysler, R. Crooks, and E. A. Starke, Jr., "Aluminium-Lithium-Alloys," ed. T. H. Sanders and E. A. Starke, Jr., TMS-AIME, Warrendale, PA, 1981, pp. 263-291.